

Medicinal Chemistry & Drug Discovery

2, 2'-Dihydroxybenzophenones and Derivatives. Efficient Synthesis and Structure Endoscopy by DFT and NMR. Credentials as Potent Antiinflammatory Agents.

Demeter Tzeli,^[b] Pawel Kozielowicz,^[c] Maria Zervou,^[d] Constantinos Potamitis,^[d] Katerina Kokkotou,^[d] Benedikt Rak,^[e] Anthi Petrou,^[f] Evaggelia Tsolaki,^[f] Antonios Gavalas,^[f] Athina Geronikaki,^[f] Ioannis D. Petsalakis,^[b] and Petros G. Tsoungas^{*,[a]}

2,2'-dihydroxybenzophenones and derivatives have been synthesized directly or by oxidation of their incipiently obtained benzylic alcohols by diverse efficient methods. Oxime and N-acyl hydrazone derivatives have also been prepared. Their structure profile has been scrutinized by DFT/B3LYP-6-311++G** methodology, NMR spectroscopy and dihedral angle grid scan analysis. Energetically favorable conformations pointed to (i) an almost coplanar bifurcated 6-membered H bridge in ketones, (ii) a single 6-membered H bridge, accompanied by a 7-membered H bonding interaction in oximes and (iii) a single 6-

membered H-bridge in hydrazones. In the latter case, a stable conformation with an additional 9-membered pseudo ring was also found. Highly deshielded protons in the NMR spectra are in accordance with the theoretically obtained findings on the H-bonded conformers. Significant anti-inflammatory activity of the compounds has been found by in vivo tests with their oxime and hydrazone derivatives showing the highest activity, hydrazone **11**, in particular, competing with marketed drugs. *In silico* docking studies point to the perspective potency of these structures as COX-1/COX-2 inhibitors.

1. Introduction

Arylketones are important building blocks in both natural products, particularly bioactive ones, drugs and functional materials.^[1] Quite a few benzophenone analogues have been scrutinized as anti-inflammatory agents.^[2,3] Most of the biologically active benzophenones^[6] are sterically crowded substrates hav-

ing substituents at *ortho* positions to the ketone moiety.^[5] Among them, natural hydroxybenzophenones,^[6,7] biologically active metabolites present in plants and especially in Guttiferae family or polyhydroxybenzophenones^[8] have displayed significant free radical scavenging activity. Substituted *ortho* hydroxybenzophenones, are ubiquitous in naturally occurring and synthetic compounds with important biological activities.^[9] Their structure and the inherent intramolecular H bonding have been the subject of extensive theoretical investigations.^[10] The *ortho*-hydroxy diaryl ketone entity in many biologically active compounds and natural products makes it a privileged structure in medicinal chemistry and a synthesis target.^[7] Well-known and important members are the combretastatins and phenstatins.^[11] Unsymmetrically substituted and congested hydroxybenzophenone derivatives have also been reported, PKA inhibitor balanol^[12] or G6Pase inhibitor mumbaistatin^[13] being two prominent examples.

Hydroxybenzophenones are not readily accessible and while numerous methods for their preparation have been described^[14,15] more are constantly in demand. It is known that the reactivity and biological activity of hydroxybenzophenones is linked to their acid-base and metal chelating properties.^[15] It is also known that their pharmacology usually works through direct interaction with metal-bearing active enzyme sites.^[16] It is reasonable to assume that the carbonyl and the *o*-hydroxyl groups are major determinants of this activity. Interestingly, a few of their carbonyl N-derivatives have been found to be more potent in this respect. Indeed, some oximes^[17] and hydrazones^[18,19] have been tested for a broad range of biological activities. A few hydrazones, particularly their N-acyl variants, exhibit anti-inflammatory activity.^[19,20] The pursuit of potent

[a] Dr. P. G. Tsoungas
Department of Biochemistry
Hellenic Pasteur Institute
127 Vas.Sofias Ave., Athens, GR-11521, Greece
E-mail: pgt@otenet.gr
pgt@pasteur.gr

[b] Dr. D. Tzeli, Dr. I. D. Petsalakis
Theoretical and Physical Chemistry Institute
National Hellenic Research Foundation
48 Vassileos Constantinou Ave., Athens 116 35, Greece

[c] P. Kozielowicz
School of Clinical and Experimental Medicine
College of Medical and Dental Sciences, University of Birmingham, Edgbaston, Birmingham B15 2TT, UK

[d] Dr. M. Zervou, Dr. C. Potamitis, K. Kokkotou
Institute of Biology, Medicinal Chemistry and Biotechnology
National Hellenic Research Foundation
48 Vassileos Constantinou Ave., Athens 116 35, Greece

[e] B. Rak
Centre for New Technologies
University of Warsaw
02-097 Warsaw, Poland

[f] A. Petrou, E. Tsolaki, Dr. A. Gavalas, Prof. A. Geronikaki
Laboratory of Pharmaceutical Chemistry
School of Pharmacy, Aristotle University of Thessaloniki
Thessaloniki 54124, Greece

Supporting information for this article is available on the WWW under <http://dx.doi.org/10.1002/slct.201600396>

NSAIDs, with a favourable ADME(T) profile^[21] compared to that of their marketed relatives, continues unabated.

Inflammation, in particular, acute or chronic, is a systemic response to an invading pathogen or injury.^[22] While the former is a short-lived physiological response to an injury, irritation or infection, the latter is a serious risk factor for the etiology of cardiovascular disease, cancer or diabetes, to name a few. An inflammatory response may be generated by complex processes and triggered by mediators such as histamine, serotonin, pro-inflammatory cytokines or arachidonic acid metabolites (e.g. prostaglandins, leukotrienes). The latter are produced through the 5-lipoxygenase pathway producing leucotrienes or the cyclooxygenase (isoforms COX-1 and COX-2) pathway producing prostaglandins (PGs).^[23] Nonsteroidal anti-inflammatory drugs (NSAIDs), therapeutics used for the treatment of inflammation, pain and pyresis,^[24] block, at least in part or suppress the formation of PGs, thus, offering relief from these symptoms. Although NSAIDs (e.g. ketoprofen, ibuprofen, naproxen, aceclofenac, diclofenac, celecoxib, etc) are among the best-selling drugs by market share in the world, they are associated with gastrointestinal and cardiovascular complications and disorders.^[23] Clearly, there is an urgent need for new chemical entities with satisfactory anti-inflammatory response and minimal side effects (particularly in the stomach and the upper GI tract).

2,2'-Dihydroxybenzophenones^[25,26] and derivatives exhibit obvious structure similarities to their above described congeners, their ring-closed analogue xanthone^[27] as well as to a few marketed drugs. The reactivity profile of xanthone^[27] and its inhibitory potential towards human glutathione S-transferase (GST)^[28,29] isoenzymes have been recently investigated. The diverse biological activity of xanthone and its relationship to its ring-opened analogue 2,2'-dihydroxybenzophenone prompted us to (a) develop efficient methods for the synthesis of 2,2'-dihydroxybenzophenones and (b) scrutinize their structure profile and a few of their oxime and hydrazone derivatives. To that end, we prepared some selected members of this class and used the DFT-B3LYP/6-311 + G** approach and an NMR experimental data-supported grid scan analysis to study their conformational features. A fundamental assessment of their anti-inflammatory potential was performed by *in vivo* tests providing valuable structure-activity relationship (SAR) feedback. *In silico* docking studies were also applied to investigate their binding properties onto the cyclooxygenase COX-1/COX-2 enzymes.

2. Results and Discussion

2.1. Chemistry

The diaryl ketone core unit of our structures is also found in the broadly used drug ketoprofen (Figure 1 A, C). A similar arrangement is found in its dialkyl nabumetone, indole-, pyrrole- or thiophene- analogues indomethacin, tometin (or ketorolac) or suprofen, respectively. An acidic site and an (hetero) aromatic hydrophobic frame, are allegedly major requisites for the observed inhibitory action of NSAIDs. Accordingly, our structures

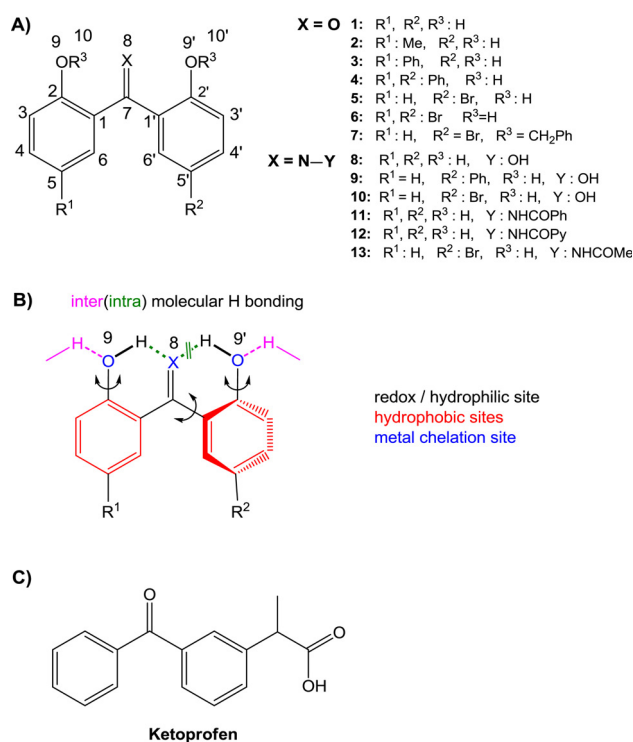


Figure 1. A) Substituted 2,2'-dihydroxybenzophenones, oxime and hydrazone derivatives. B) Interaction sites of ketones 1–6 and N-derivatives 8–13 C) Ketoprofen.

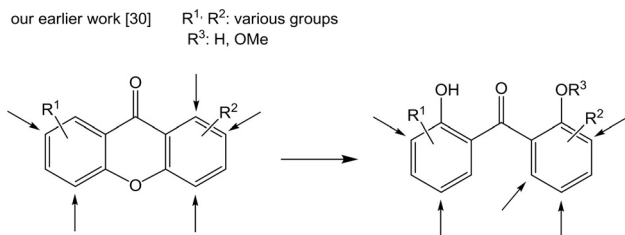
were assembled by adopting the ligand-based design approach.^[30] Thus, introducing OH groups at *ortho* positions to the pivot carbonyl centre we engender (a) acid-base (i.e., redox) properties, (b) metal-chelating properties, (c) H bonding (intra- and/or intermolecular) interactions and (d) further derivatization potential (Figure 1B). An advantage of our structures, over those of marketed anti-inflammatory drugs rests upon the acidic sites of the former (variable by substitution), particularly their oxime or *N*-acyl hydrazone derivatives, in place of an acid group, present in most marketed drugs. It is this group that is incriminated for their insulting effects (mainly to the GI tract). Our structures are, thus, expected to minimize the adverse side effects while keeping a competent anti-inflammatory profile. On the other hand, *p*-substitution of weak electronic influence, yet of steric ramifications, has been selected to enable a clear elucidation of the impact of these elements (essential to a pharmacology profile) onto the geometry of the structures and consequently their anti-inflammatory potential.

2.1.1. Synthesis

Unlike various methods available for the synthesis of hydroxybenzophenones, their *ortho*-dihydroxy- counterparts have not enjoyed a similar attention. Yet, these potentially amphiphilic structures are a target and a challenge for both chemistry and biology.

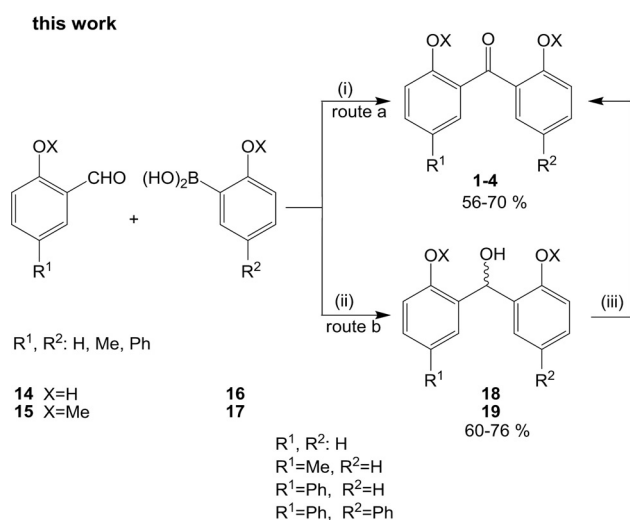
An approach for the construction of the core structure 1 and various derivatives, 2–13 among them (Fig. 1A), from the

ring cleavage of suitably substituted xanthenes (Scheme 1), has been recently reported.^[14,25]



Scheme 1. Substituted Xanthenes.

For the objectives in hand, alternative efficient protocols for the synthesis of our target structures **1–4** have been devised and are described herein. Accordingly, the appropriately substituted components are assembled, either *directly* (Schemes 2 and 3, route a) or *indirectly* by way of benzylic alcohol derivatives **18** or **19** (Schemes 2 and 3, route b). The key reaction of the protocol laid out in Scheme 2 is the coupling of the alde-

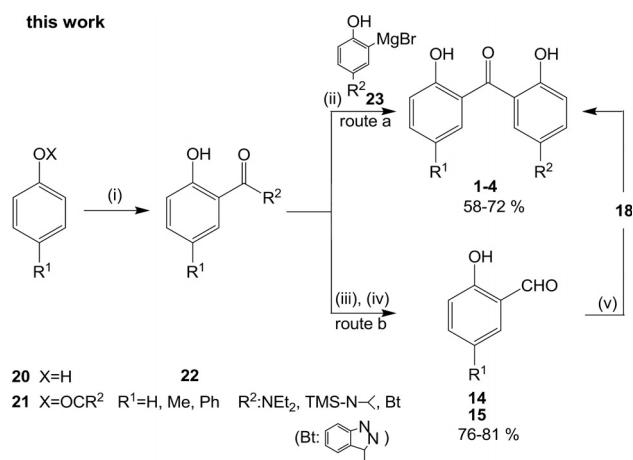


Scheme 2. Reagents and conditions: (i) $[Rh(CH_2)_2Cl]_2P^tBu_3$, 80 °C, 1,4-dioxane:acetone (4:1) [Ref. 35] (route a); (ii) $RhCl_3 \cdot 3H_2O$, imidazolium chloride, DME, NaOMe, 80 °C [Ref. 39] or $Cu(OAc)_2$, dppf, NaOAc, toluene, reflux [Ref. 40] (route b); (iii) (a), KI, K_2CO_3 in H_2O or in $tBuOH$ [Ref. 38] or (b) PCC, dry DCM, 0 °C then 10 °C 6 h, r.t. 6 h [Ref. 37] or (c) oxone, TEMPO/ $n-Bu_4NBr$ [Ref. 36].

hyde **14** (or **15**) with the boronic acid **16** (or **17**) (Scheme 2, routes a or b). A ligand-free Pd-catalyzed C–H arylation of aldehydes of type **14** with boronic acids is known to furnish hydroxybenzophenones directly.^[31] Our aldehyde **14** (or **15**) has been prepared by an *ortho*-formylation of the corresponding phenol^[32,33] (Scheme 2). Of the vast number of methods available for the synthesis of boronic acids, **16** was conveniently prepared by an electrophilic borylation of the appropriate

Grignard component, in accord with a recent report.^[34] Then, a Rh-catalyzed C-arylation of aldehyde **14** (or **15**) with the *O*-methyl protected boronic acid **17** gave ketones **1–4** directly (Scheme 2, route a).^[35] It was found that using this method, **1–3** could also be obtained directly from **14** and **16** (i.e., without OH protection) whereas **4** was indirectly prepared *via* the oxidation of its corresponding alcohol **18**.^[36–38] A C–H arylation of **14**, either Rh-catalyzed^[39] or Cu-catalyzed,^[40] has also been carried out, under simpler and more gentle reaction conditions. Both reactions, however, pay the toll of an additional step, i.e., that going through the intermediate benzylic alcohol precursor **18**,^[41] oxidation of which,^[36–38] ultimately, gave **1–4** (Scheme 2, route b). The PCC- and iodine-based^[37,38] oxidations of **18** are preferable, as they proceed readily and efficiently, under mild conditions (see experimental). The adopted methods have been chosen to avert any *o*- and/or *p*-quinone formation, particularly for the vulnerable unsubstituted alcohol leading to **1**. On the other hand, the formation of **2–4** is not in danger of a concomitant phenol *p*-oxidation, having that position blocked with non-readily oxidizable groups. *o*-Oxidation of the phenol rings is also deterred by a Resonance-Assisted H Bonding (RAHB)-pseudo ring stabilization (see later section 2) of a phenoxyl radical, should that be transiently generated (see section 2.1.3).

Alternatively, a versatile protocol (Scheme 3) takes advantage of either an amide acylation or an anionic *ortho*-Fries re-



Scheme 3. Reagents and conditions: (i) LDA (or *s*-BuLi/TMEDA), THF, –78 °C, NH_4Cl [Ref. 42]; (ii) **30**, THF, N_2 , 8–12 h, NH_4Cl [Ref. 7] (route a); (iii) $Cp_2ZrCl_2 \cdot LiAlH(O^tBu)_3$ (Schwartz reagent), THF, r.t. [Ref. 44] (route b); or (iv) DMF, NaOH, EtOH-Et₂O (1:1), r.t., 3 h [Ref. 43]; (v) as in Scheme 2.

arrangement and an amide reduction to an aldehyde as the key reactions. Thus, amide **22**, directly acylated with Grignard component **23** (route a)^[7] or reduced by in situ prepared Schwartz reagent ($Cp_2ZrCl_2/LiAl(O^tBu)_3$) (route b)^[41] to the aldehyde **14**, ultimately led to **1–4**. **22** was conveniently obtained by lithiation of the carbamate **21** followed either by an anionic *ortho*-Fries rearrangement^[43] (route b, (iii)) or its in situ further treatment^[44] (route b, (iv)) to **14**. It should be noted that

both formylation methods can be tuned into a one-pot transformation. Of interest is the use of benzotriazole in **20**, as a readily migrating amine in this rearrangement, like other commonly employed aliphatic or alicyclic amines.^[43] Its use was inspired by (a) the engagement of tetrazole in anionic *ortho*-Fries rearrangements^[44] and (b) its engagement as an organocatalyst in transamidation reactions.^[45]

While the delineated Schemes 2 and 3 include efficient individual operations and allow substrate compatibility, the OH protection and deprotection steps, if dictated by the substitution pattern in either or both reacting partners (as **15** and **17**), may intervene as an impediment to the overall efficiency of the reaction sequences. In that case, mild O-demethylation in the ultimate step, if needed, can be effected by magnesium iodide etherate (MgI₂-OEt₂) in preference to the commonly used BBr₃.^[46] In this context, Scheme 3 (routes a and b) offers a more convenient and cost effective alternative to the synthesis of **1–4**.

On the other hand, precedents suggest that an intramolecular H bonding by the *o*-OH group in aldehydes **14** or **15**^[47] or in amide **22**^[43] not only affects their innate reactivity, as it appears to facilitate the C-arylation (Schemes 2 and 3, routes b) or C-acylation (Scheme 3, route a), respectively, it also protects the OH group, thus, obviating a protection-deprotection protocol.

1 was also benzylated on both OH groups^[25] to give **7**. The latter were preferred over their chemically robust O-methyl derivatives for the biological activity experiments described herein, merely due to the usefulness of the benzyl group as an "arming" entity in biology^[48] (see later).

The oximes **8–10** and *N*-acyl hydrazones **11–13** were prepared directly from **1** (i.e., without a OH protection-deprotection protocol), following earlier reported procedures.^[25]

It is of significance to note that the applied protocols in Schemes 2 and 3 provide a means to differentiate between two otherwise identical aromatic rings and OH groups in the parent structure **1** and, thus, allow the synthesis of a diverse array of useful derivatives through further transformations.

2.1.2. Structure Profile

Some basic features of the structure of ketones **1–7**, as well as their oxime **8–10** and *N*-acyl hydrazone **11–13** derivatives, we have briefly touched upon, recently.^[14] What all structures **1–13** (Figure 1) have in common is a molecular framework of a pivot C=X moiety [**1–7**, X=O; **8–10**, X=NOH; **11–13**, X=HN(COPh)(Py)(Me)] bridging two *o*-hydroxy-substituted aryl rings. Their features not only attest to their identity but have ramifications of broader impact on such aspects as (a) the Resonance-Assisted H Bonding - directed intramolecular H bonding (RAHB-directed IHB) or (b) the intrinsic strength of O–H...O / N bonding, rationalized by the difference in the inherent proton affinities (PA) of O and N atoms.^[49] Rotation of the rings about the pivot moiety gives rise to various energetically (un)conformations (see Figs.1S–2S of Supporting Information (SI)). The chelate (through IHB) arrangements facilitate the proximity of the bonding donor (O–H) and acceptor (O or N) participants

and confer stability to the conformation. The conformation assumed by all structures is a twisted one, in which the two rings are not coplanar. Variations in the *ipso* and *ortho* bond lengths and angles reflect the H bonding impact on the ring π re-distribution.

The calculated selected geometries are given in Tables 1S–3S of the SI, conformation barriers between the non bonded ("open"), singly bonded and bifurcated ("closed") conformers are given in Table 4S of the SI.

2D ROESY spectroscopy has been applied to unveil the conformational features of the structures in solution, particularly the potential of a H bridge-derived pseudo ring (see following sections). Chemical shifts and assignments are given in Tables 1–3 (see below and also Figure 13S–21S of the SI). The data were acquired in CDCl₃ to avoid or minimize solvent-mediated intermolecular H bonds, except where solubility problems imposed the use of DMSO. A grid scan search explored their energy mapping laid out by a systematic variation of the crucial dihedral angles 2–1–7–8 (τ 1) and 2'-1'-7-8 (τ 2), defining the orientation of the two phenol rings around the rigid central functionality. Experimental information from dipole-dipole interactions (ROE data) was used to rank the energetically favourable conformations (Fig.3S–7S, 9S–12S of the SI).

The structure of the parent **1** has been investigated by X-ray crystallography,^[50] NMR (¹H, ¹³C and ¹⁷O)^[51] and FT-IR spectroscopy^[52] as well as DFT–B3LYP/6-31G* calculations.^[53]

1 exhibits a lower than C₂ symmetry with a deviation from planarity sterically triggered by the relative orientation of the aryl rings.^[50] We have, indeed, verified it by our DFT–B3LYP/6-311++G** geometry optimized calculations on the ketones **1–7** (parent **1** is included as the reference structure). The calculated IHB distances, angles and dihedral angles involving H bridge are given in Tables 1S–3S of the SI. Indeed, the carbonyl and the hydroxyl groups are set to develop non equivalent IHBs. A notable twist angle of ca. 43–44° has been found between the aromatic rings leading to a non planar conformation. Earlier calculations for **1**, using smaller basis sets, have estimated this angle at ca. 23°^[53] or ca. 52°^[50,54] against an X ray-determined one of ca. 38°.^[50] The non planar arrangement and resulting distortion cannot impede bifurcation (Figure 2). Data on mono-hydroxy analogue^[55] are shown in Table 1S of the SI for comparison.

IHB is known to stabilize a conformation, through an RAHB^[56] 6-membered *pseudo* (quasi) ring, by conjugation with a π -density. Vibrational frequencies^[57] and electron distribution^[58,59] of this stabilization type in *pseudo*-ring conformations have been measured. In general, weak bifurcated H bonds become stronger by intramolecular RAHB.^[56–59]

Monosubstitution, as in **2**, **3** and **5** or disubstitution, as in **4**, carrying a higher strain cost or with a weak electron withdrawing effect, as in **6**, do not trigger an appreciable distortion of the structures. In the bifurcation region of **1–6** two O...H bonds stretch in the range of 1.717–1.724 Å (Table 1S of the SI). A slight deviation (ca. 0.05 Å) from the average 1.491 Å value for **1–7** (or **1'-7**) bond is indicative of a RAHB-promoted π -conjugation between the H-bonded *pseudo* and the phenol rings. Deviations from planarity for the two rings, range from ca.

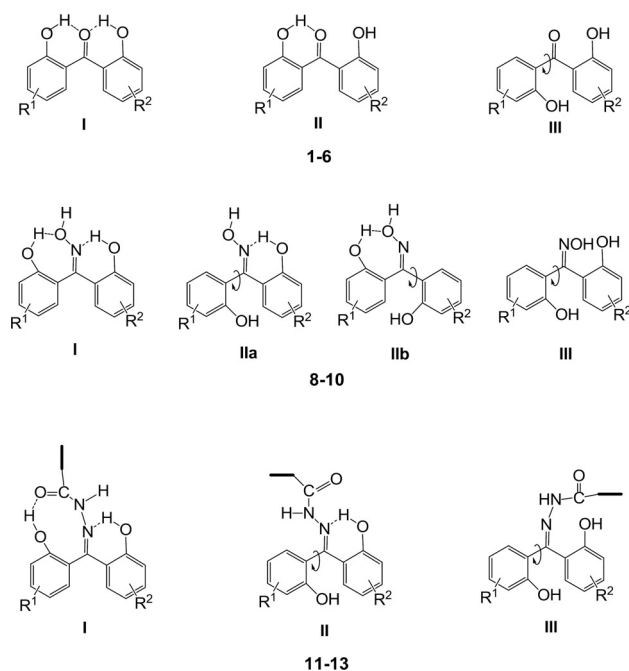


Figure 2. RAHB pseudo ring conformations: left column (type I, bifurcated), middle column (type II, singly H bonded conformation) and right column (type III, non H bonded conformation).

conformation flexibility. Thus, an elongation (*ca.* 0.02–0.04 Å) of all bonds forming the *pseudo* ring is observed. Indicative of the inherent distortion are also the 1–7–1' and *ipso* 1–2–9' (or 1'–2'–9') angles of 123° and a rather subtle (*ca.* 0.01 Å) displacement of C-7 from the 8–1–1' plane.

Grid scan analysis for **1** and **4** indicated the free rotation of the two phenol rings around the central ketone moiety. Thus, apart from the coplanar orientation of the two phenol rings, all the other configurations of the dihedrals are favored while certain conformers can develop H bonding between the ketone and the hydroxyl groups. The derived energy contour plots and representative conformational minima are shown for **1** and **4** (Figure S5 and S4, SI).

¹H NMR chemical shifts for the mono-substituted **3** and **5** display two deshielded OH resonances at 10.40 and 10.66 ppm, (see Table 1), indicative of a bifurcated H bridge in the RAHB-stabilized *pseudo* ring, in line with the calculated geometry data. This is further supported by 2D spectroscopic data in the case of **3**, where the observed ROE interaction between the phenyl protons H₆ and H_{6'} necessitates the positioning of the OHs towards the same space as the ketone moiety. Thus, although the grid scan analysis allows the unhindered rotation of the two rings around the central dihedrals τ_1 and τ_2 (see Fig-

Table 1. NMR chemical shifts and assignment of the ketones **1**, **3**, **4** and **5**.

	1 [§]		3 [§]		4		5 [§]	
	¹ H	¹³ C	¹ H	¹³ C	¹ H	¹³ C	¹ H	¹³ C
3	7.48 (d, 8.3 Hz)	120.6	7.18 (d, 8.6 Hz)	121.7	7.55 (d, 8.7 Hz)	121.13	7.10 (d, 8.4 Hz)	121.46
3'			7.12 (d, 8.3 Hz)	121.3			7.00 (d, 9.0 Hz)	123.13
4	7.74 (t, 7.6 Hz)	137.5	7.77 (dd, 8.6, 1.9 Hz)	137.2	7.95 (dd, 8.7, 2.4 Hz)	136.16	7.55 (t, 8.0 Hz)	139.15
4'			7.54 (t, 8.3 Hz)	138.7			7.60 (d, 8.31 Hz)	135.31
5	7.37 (t, 7.5 Hz)	126.5	-	-			6.99 (t, 7.5 Hz)	121.83
5'			6.96 (t, 7.5 Hz)	121.6			-	-
6	8.34 (dd, 7.9, 1.4 Hz)	129.3	7.82 (d, 1.9 Hz)	133.71	8.56 (d, 2.2 Hz)	127.14	7.59 (d, 8.81 Hz)	141.09
6'			7.69 (d, 7.9 Hz)	135.56			7.72 (d, 2.2 Hz)	137.40
9/13 (9'/13')			7.51 (d, 8.3 Hz)	129.14	7.68 (dd, 8.34, 1.13 Hz)	129.62		
10/12 (10'/12')			7.43 (t, 7.6 Hz)	131.5	7.48 (t, 7.7 Hz)	131.58		
11 (11')			7.34 (t, 7.3 Hz)	129.9	7.38 (dd, 10.6, 4.2 Hz)	130.45		
Ar-OHs			10.66 (s)				10.41 (s)	
			10.51 (s)				10.49 (s)	
solvent	CDCl ₃							

[§]Chemical shifts without the assignment of compounds **1**, **3** and **5** have been reported in ref. 16.

0.03 Å to 0.09 Å. Comparing the H bonding of **1–6** with that in 2-hydroxy-benzophenones^[7,10] or tricyclic planar anthralin^[54] (Table 1 of the SI), one can see the effects of bifurcation on

ure S5 SI), NMR data clearly support the formation of a bifurcation bridge.

Table 2. NMR chemical shifts and assignment of the oximes **8** and **10**

¹ H	¹³ C	¹ H ^a	¹³ C ^b			
1			120.14	120.45		
1'			123.40	122.45		
2			159.65	155.56		
2'			155.43	158.83		
3	7.06 (d, 8.25 Hz)	120.55	6.96 (d, 8.2 Hz)	133.1	7.03 (d, 8.2 Hz)	132.33
3'	7.02 (dd, 8.3, 0.9 Hz)	119.94	6.91 (d, 8.8 Hz)	122.1	6.83 (d, 8.8 Hz)	121.67
4	7.39(t, 7.7 Hz)	134.37	7.24 (t, 7.24 Hz)	122.6	7.39 (ddd, 8.6, 7.0, 3.9 Hz)	123.86
4'	7.27 (t, 7.8 Hz)	134.25	7.45 (dd, 8.8, 2.4 Hz)	136.86	7.29 (dd, 8.7, 2.4 Hz)	136.64
5	7.04 (t, 7.2 Hz)	123.54	6.81 (t, 7.44 Hz)	134.4	7.06 (t)	134.4
5'	6.79 (dd, 7.6, 0.9 Hz)	122.1	-	115.43	-	114.16
6	7.11(dd, 7.6, 1.6 Hz)	132.6	6.89 (dd, 8.0, 1.3 Hz)	119.8	7.07 (d, 8.10 Hz)	120.35
6'	6.92 (dd, 8.0, 1.5 Hz)	133.51	7.21 (d, 2.3 Hz)	134.83	6.98 (d, 2.3 Hz)	135.37
7				160.7		161.4
Ar-OHs	-					
solvent	CDCl ₃					

^s Chemical shifts and assignment of **8** in DMSO have been reported in ref. 30. ^{a,b}, Two sets of NMR resonances of **10** were observed.

Replacing O by N in the pivot double bond (i.e., 7–8 bond), forces the conformation to non equivalent H bonding arrangements in oximes **8–10**. Oximes are known to function as H bond donors, through their OH site and acceptors, through their N lone pair.^[60] A repulsion develops among the directly bonded sp² N and O lone pairs in the planar NOH entity and this is a major determinant of their preferred conformation.^[61] It can be safely assumed that it is (a) the sp² N, forming the RAHB-stabilized 6-membered chelate ring and (b) the enhanced oxime O lone pair availability (N–O lone pair repulsion-driven, reminiscent of the α effect)^[62,63] that give rise to the alternative conformation and H bonding interactions. The N and O lone pair repulsion, augmented by the presence of two identical phenol rings in **8**, slightly modified by 5-substitution (as in **9** and **10**), (a) engenders the donor-acceptor character to the oxime O site and (b) forces one of the rings out of planarity by a substantial deviation. Both dictate their preferred conformation, as demonstrated by twist angles of ca. 69–70° (Figure 2, I and Tables 2S and 3S of the SI). In this class, the IHB of the 8–10 bond remains while a new 7-membered *pseudo* ring-forming H bonding of ca. 1.878 Å length (10'-11 bond, Figure 2, I or IIb and Table 1S of the SI) builds up between the oxime O site and that of the unsubstituted ring. The 8–10 bond (O–H...N) of ca. 1.741 Å in **1–6** is expectedly slightly weaker (ca. 0.02 Å) than its O-counterpart. Slight deviations (ca. 0.01–0.02 Å) from the typical 1.491 Å value for 1–7 and 1'-7' bonds, respectively, indicate the non-equivalence of these bonds. A ca. 2.602 Å 8–9 (N–O) distance of the H bridge is in agreement with the generally observed range of 2.51–2.65 Å for the oximes.^[61] This distance, is closer to aldoximes (ca. 2.63 Å) compared to ketoximes (ca. 2.52 Å).^[61] On the contrary, the 8–9' (N–O) distance of ca. 3.16 Å is expectedly way longer than the

commonly observed in 6-membered chelate ring formations. Most interesting, however, is an elongation found for the 7–8 (C=N) bond (Table 1S of the SI) that compares satisfactorily with the upper end of the generally found range of 1.27–1.29 Å in oximes.^[61] The 1–7-1' angles are ca. 120.5°, matching those of analogous ketoximes.^[61] Other bond angles as well as dihedral ones (Tables 2S, 3S and 5S of the SI) are indicative of the inherent distortion and the relatively loosely formed *pseudo* rings.

The NMR data of **8**, in contrast to its parent **1**, display the symmetrical protons of the two rings as magnetically non equivalent (Table 2). This is attributed to the restricted rotation around the C=N bond of the oxime moiety, which “locks”

its OH group in a certain orientation towards one of the two phenol rings, thus, inducing different magnetic environments to their protons. Moreover the “locked” orientation of the oxime OH imposes an energy barrier of ca. 8 kcalmol⁻¹ hindering the free rotation of the phenol ring (Figure 7S SI). DFT calculations have estimated barriers of ca. 13–14 kcalmol⁻¹ (see section 2.1.3). Grid scan analysis also highlighted the possibility of H bonding between the phenol OHs, though such H bonding was not confirmed by the NMR data.

Interestingly, two sets of NMR signals were observed for **10** in a population ratio 1:1, indicating the presence of two distinct conformations (Table 6). This is attributed to a symmetry disruption by bromine substitution. This point is further confirmed by an array of ¹H NMR spectra acquired in a temperature range 25–80°C, where no coalescence of the “brothered” peaks was observed (Figure 8S, SI). The ROE interaction observed between H₆ and H_{6'} protons (at least for one conformer) is in accordance with the orientation of the phenol OHs towards the same space relative to the oxime group. Grid scan analysis supports the existence of two conformations and reveals the possibility of H bonding between the phenol OH and the oxime N site (Figure 9S, SI), in concert with DFT data.

Geometry features, similar, in part, to those of oximes **8–10**, are more pronounced in hydrazones **11–13** (Tables 1S–3S and 5S of the SI). The two rings are markedly twisted out of planarity by ca. 60–73°. A single RAHB-stabilized 6-membered chelate ring is clearly formed whereas the pendant N-acyl arm, through a sterically favourable orientation (Figure 2), gives rise to what appears to be a 9-membered *pseudo* ring-like interaction.

The changes in these bonds reflect the RAHB impact on the ring π distribution,^[56,57] engaging only the substituted ring.

Table 3. NMR chemical shifts and assignment of the Hydrazones 11–13

		11^s		12		13^{a,b}			
	¹ H	¹³ C	¹ H	¹³ C	¹ H ^a	¹³ C ^a	¹ H ^b	¹³ C ^b	
	3	6.95 (d, 8.1 Hz)	117.55	6.95 (d, 8.1 Hz)	120.2	7.03 (d, 8.2 Hz)	119.6	6.88 (d, 8.8 Hz)	122.4
	3'	7.06 (d, 8.3 Hz)	117.13	7.05 (d, 8.2 Hz)	119.7	6.96 (d, 8.8 Hz)	121.7	6.87 (d, 8.1 Hz)	120.2
	4	7.26 (t, 7.6 Hz)	131.58	7.26 (t, 7.4 Hz)	134.2	7.40 (t, 7.8 Hz)	134.7	7.21 (t, 7.7 Hz)	133.7
	4'	7.39 (t, 7.4 Hz)	132.00	7.38 (t, 7.2 Hz)	134.7	7.52 (dd, 8.7, 2.4 Hz)	136.9	7.35 (dd, 8.7, 2.5 Hz)	135.9
	5	6.74 (t, 7.5 Hz)	119.00	6.74 (t, 7.4 Hz)	121.5	6.98 (t, 7.7 Hz)	122.7	6.71 (t, 7.5 Hz)	121.6
	5'	6.99 (t, 7.4 Hz)	120.03	6.98 (t, 7.4 Hz)	122.6	-	-	-	-
	6	6.80 (d, 7.5 Hz)	130.55	6.79 (d, 7.6 Hz)	133.3	7.09 (d, 7.4 Hz)	132.6	6.64 (d, 6.4 Hz)	132.4
	6'	7.17 (dd, 7.5, 1.1 Hz)	130.55	7.16 (d, 6.8 Hz)	132.9	7.26 (d, 2.4 Hz)	134.8	6.69 (d, 2.4 Hz)	134.2
	9	-	-	-	-	1.97(s)	24.12	1.97(s)	24.12
	10	7.61 (d, 7.0 Hz)	128.15	8 (d, J = 7.7 Hz)	139	-	-	-	-
	11	7.45 (t, 7.6 Hz)	129.03	7.51-7.46 (m)	126.8	-	-	-	-
	12	7.54 (t, 7.4 Hz)	132.48	-	-	-	-	-	-
	13	7.45 (t, 7.6 Hz)	129.03	8.16 (d, J = 8.3 Hz)	138.2	-	-	-	-
	14	7.61 (d, 7.0 Hz)	128.15	-	-	-	-	-	-
	-NH	10.15 (br.s)	-	10.07 (br.s)	-	9.94 (br.s) or 10.1 (br.s)	-	-	-
	-OHs	10.47 (s)	-	10.97 (s)	-	10.54(s) or 10.55(s)	-	-	-
		12.97(s)	-	13 (s)	-	13.18(s) or 12.94(s)	-	-	-
	solvent	DMSO	-	-	-	-	-	-	-

^s Chemical shifts without the assignment of 11 have been reported in ref. 16. ^{a,b} Two sets of NMR resonances of 13 were observed.

Substitution, in this case too, does not have a notable effect on their geometry. Worth noting, however, is that **12** appears to be the most markedly affected. The extent of the *pseudo* ring RAHB-driven distortion of the structures is more clearly indicated by their sharper dihedral angles whereas ring angles are similar to those found in **8–10**.

Hydrazones **11** and **12** display their symmetrical phenol ring protons as magnetically non equivalent (Table 3), a feature attributable to the *N*-acyl arm. The possibility of intramolecular H bonding is probed by the two deshielded ¹H NMR resonances in the range 10.5–13.2 ppm (Table 3). In line with this observation, grid scan analysis for **11** and **12** (Figure 10S and 11S, SI) reveals the possibility of H bonding between the phenol OH and the hydrazone *N* site. The results are in agreement with the DFT calculations, confirming the potential of a 6-membered *pseudo* ring formation.

The bromo-substituted **13**, analogous to oxime **10**, displays two sets of NMR resonances in a population ratio 1:1, thus, unveiling the presence of two distinct hydrazone conformations. As in the case of analogues **11** and **12**, the deshielded OH resonances indicate a H bonding bridge, further supported by grid scan analysis, that favours the contact between a phenol OH and the *N* hydrazone site. (Figure 12S, SI).

Relative enthalpies, Gibbs free Energies and conformation barriers (Δ_{RB}) from the non bonded (“open”, type III) to singly bonded (type II) and bifurcated (“closed”, type I) conformers (see Figure 2) are given in Table 4S of the SI and depicted in

Figure 3. The bifurcated conformation (“closed” form, Figure 2 type I) is more stable than its singly H-bonded and non-bond-

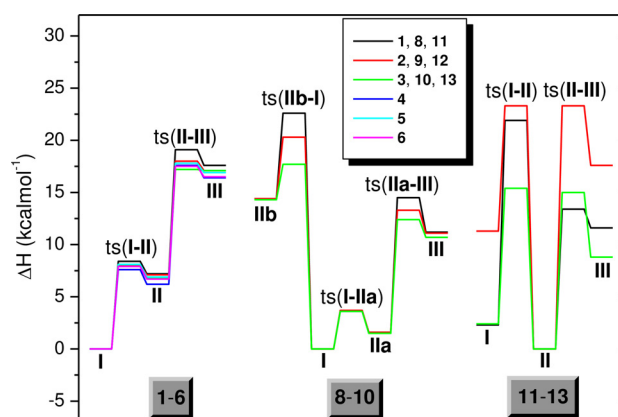


Figure 3. Enthalpy diagram of the conformer change for 1–6 and 8–13.

ed variants (semi- or fully- “open” forms, Figure 2 types II and III) for 1–10. The calculated I, II, and III conformers for all compounds are shown in Fig.2S of the Supporting Information.

The parent **1** is the most stable of all by ca. 17–18 kcalmol⁻¹ for the transition from type III to I conformation (Table 4S of the SI). The formation of a single H bond requires ca. < 3 kcal-

mol⁻¹ via the transition III to II followed by another *ca.* 1.2 kcalmol⁻¹ to bifurcation via the transition II to I. Mono-substituted **2**, **3** and **5** have a lower conformation change barrier from their di-substituted congeners **4** and **6** of *ca.* 0.5 kcalmol⁻¹ for both transitions (see Figure 3). The activation enthalpy barrier in going from III to IIa in **8–10** is less than 3.5 kcalmol⁻¹, from IIa to I is *ca.* 3.6 kcalmol⁻¹ for all while from IIb to I climbs up to *ca.* 8.2 kcalmol⁻¹. For **11–13**, the lowest energy conformer is of type II (see Figure 2). The transition from the non H-bonded to the most stable H-bonded conformer, requires an energy demanding rotation of the NNC(Ar/R)arm. Accordingly, their activation enthalpy barriers reach up to *ca.* 6.2 kcalmol⁻¹ for the conversion of type III to II. For **11–12**, a conversion from II to I is *ca.* 23 kcalmol⁻¹ while for **13** drops significantly to 15 kcalmol⁻¹.

Overall, similar relative enthalpies and activation barriers of types I–III, are observed for **1–6** (see Figure 3). Some differences, mainly in the activation barrier from IIb to I are noted in **8–10** while there are significant enthalpy differences among **11–13** (see Figure 3).

2.2. Biological Profile

The competence of benzophenone analogues as anti-inflammatory agents is well recognized.^[19,20,64] Several attempts to derive COX-selective inhibitors from benzophenone analogues have been published.^[19] A chemical insight into the inflammation mechanisms and treatment has been reported.^[22]

Prediction of the anti-inflammatory as well as antioxidant activity of **1–13** was performed using PASS12 software.^[65,66] The prediction outcome is presented as a list of activities (Table 4)

Table 4. Experimental and predicted anti-inflammatory and antioxidant activities as well as lipophilicity.				
Compounds	Antiinflammatory activity (CPE %) ^a	DPPH, (%)	cLogP ^c	Pa ^d Antiinfl/antiox.
1	Nt ^b	36.5	4.46	0.639
3	45.5	Nt	4.72	0.6/0.39
4	Nt	0.6	5.43	0.612
5	Nt	Nt	5.95	0.334/ 0.243
6	Nt	NT	7.84	0.265
7	53.56	1.4	2.28	0.252/ 0.133
8	59.66	1.6	4.17	0.525/ 0.185
9	Nt	Nt	3.59	0.438
10	58.53	1.35	3.33	0.281
11	65.76	3.7	3.64	0.201/ 0.132
12	53.0	Nt	4.77	0.232
13	38.25	Nt	4.11	0.156
indomethacin	47	98		

^a% inhibition of edema ^bNt –not tested: ^ccLogP- calculated lipophilicity: ^dPa – probability to be active

with appropriate Pa (i.e. the probability estimates to be active). An important criterion for selecting the most promising compounds is their novelty. If the Pa value is high, e.g. Pa > 0.7, one may often find a close analogy to known pharmaceutical agents but if Pa < 0.7, then the chance to find activity in experiment is diminished. However, for a compound that bears no similarity to known pharmaceutical agents, the less its Pa value the more its chance to be a new chemical entity (NCE).^[65] This is the case of **7**, **11** and **12**, which may be classified as NCEs, since, despite their prediction values of < 0.3, their considerable activity was experimentally confirmed (Table 4).

In running primary investigations, the number of derivatives submitted to testing has been kept to a minimum trying to save valuable livestock and reagents.

2.2.1. In vivo Antiinflammatory Activity

Results of this study, using the model of carrageenin-induced mouse paw edema, are presented in Table 4. Most of them showed significant anti-inflammatory action administered at a dose of 0.01mmol/kg. Compounds **11**, **8** and **10** were found to be the most potent anti-inflammatory agents of this series and the highest activity was observed for **11**. On the other hand, **13** was found to have the lowest activity. Of interest is an anti-inflammatory activity of similar magnitude exhibited by hydrazone **12** and ketone **7** (Table 4). Under the same conditions the inhibition of indomethacin protected from carrageenin induced mouse paw edema was 47%.

To assess their lipophilicity, generally taken as a potency predictor,^[67] cLogP was calculated (Table 4) using ChemDraw program. No correlation was found between anti-inflammatory activity and lipophilicity, bearing in mind the important role of the latter in drug activity (see also ref. 26).

2.2.2. In silico docking studies

Docking studies onto COX-1 and COX-2 have been performed to evaluate the binding affinity and map the interactions of representative compounds (**8**, **10**, **11**). The crystal structures of COX-1 in complex with flurbiprofen (PDB code 1EQH)^[68] and COX-2 co-crystallized with diclofenac (PDB code 1PXX)^[69] were used as templates.

In the crystal complex of COX-1 with flurbiprofen the crucial residues Arg120 and Tyr355 develop H-bonds with the ligand while the residues Val349, Leu352, Trp387, Ala527 and Ser530 are involved in lipophilic interactions. In the case of COX-2 crystal structure, diclofenac contacts through H-bonds Ser530 and Tyr385 while a number of lipophilic interactions are developed with Val349, Val523, Gly526, Ala527, Leu531 and Trp387.

The results derived from a best-ranked scoring pose for compounds **8**, **10** and **11** are presented in Figures 4-5 and reported in Tables 5 and 6. In the case of COX-1, the oximes **8** and **10** seem capable to interact with the crucial residue Tyr355 through H-bonding. Interestingly, the docking pose of **8** favours the formation of an intramolecular H-bond as also supported by our theoretical studies resulting to 6-member pseu-

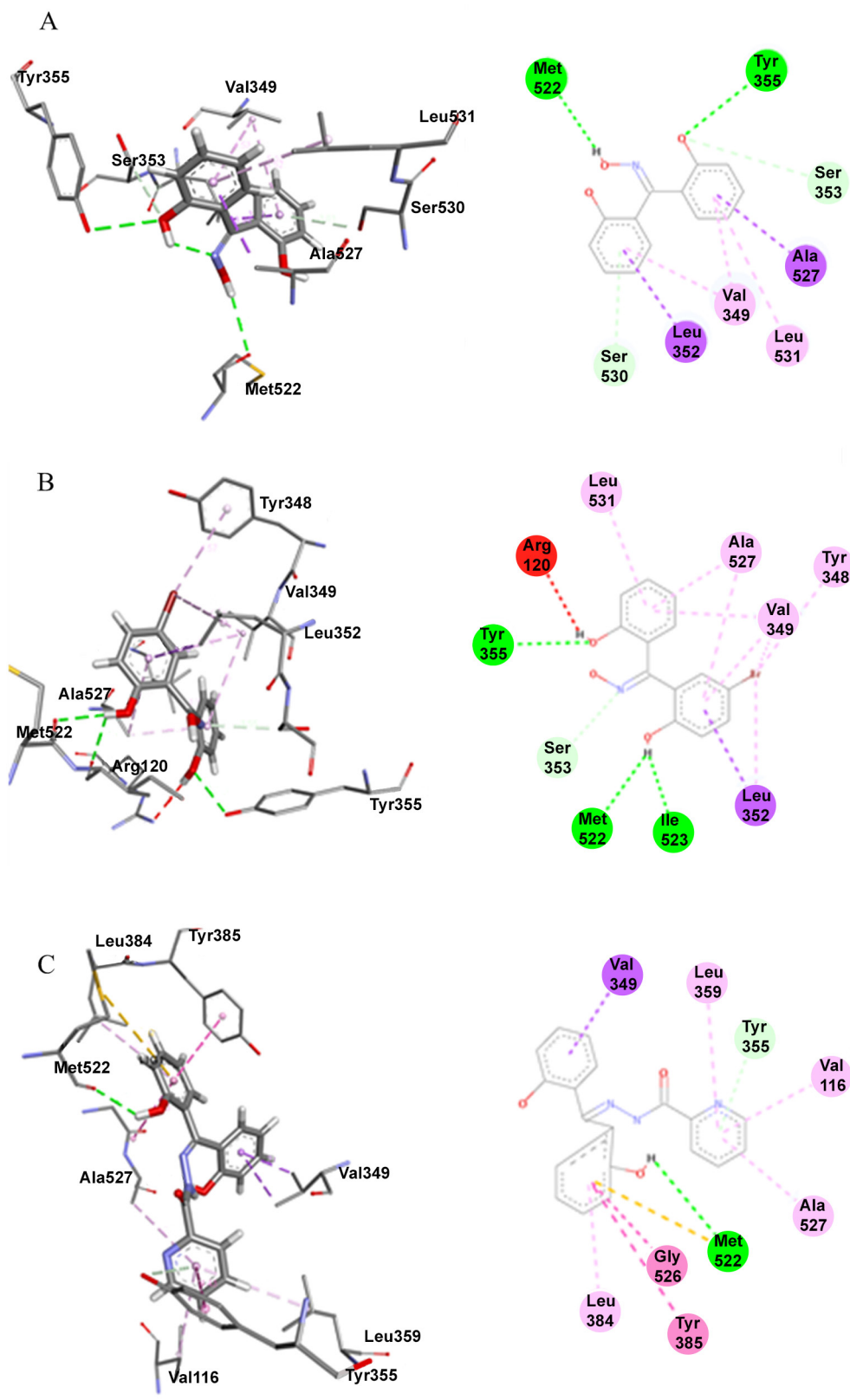


Figure 4. Docking poses of **8** (A), **10** (B) and **11**(C) at COX-1 binding site along with their interactions. H-bonds and hydrophobic interactions are indicated with green and purple dotted lines, respectively.

do ring which bridges Tyr355 and Met522. Regarding COX-2, compound **8** contacts through two H-bonds the crucial residue Ser530 and forms one additional H-bonding with residue Gly526 while it develops hydrophobic interactions with the crucial

residues Val349, Trp387, Val523, Ala527, Leu531 as well as with Leu352. Compound **10**, interacts mainly through H-bonding with Met522 as well as halogen bonding with Tyr385 and through lipophilic interactions with Val349, Ala527 and Leu531.

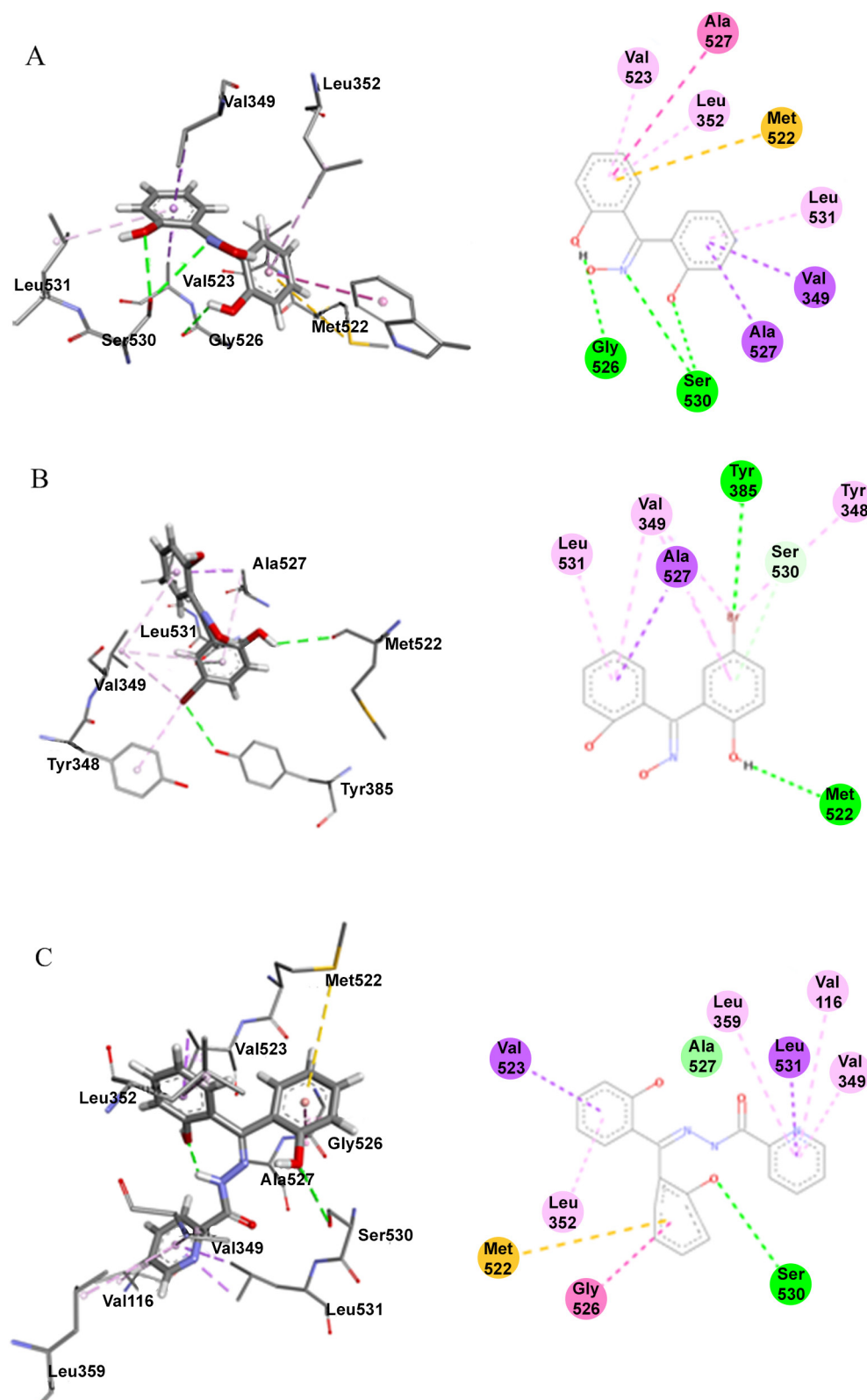


Figure 5. Docking poses of **8** (A), **10** (B) and **11**(C) at COX-2 binding site along with their interactions. H-bonds and hydrophobic interactions are indicated with green and purple dotted lines, respectively.

Compound **11** bearing the most potent anti-inflammatory activity exhibits the best predicted binding affinity in both COX-1 and COX-2 enzymes. The binding at both receptors is governed mainly by lipophilic interactions between the aromatic rings of

the ligand and the crucial amino acids Val349, Ala527 and Tyr355, of COX-1 and Val349, Val523, Gly526, Ala527 and Leu531 of COX-2. Moreover, **11** develops H-bonding with Met522 at COX-1 and with the crucial residue Ser530 at COX-2.

Table 5. COX-1 1EQH binding affinities.

compound	Est. binding energy (kcal/mol)	Binding affinity score	RESIDUES of the active site participating in H-bonds
8	-7.9	-34.22	Tyr355, Met522
10	-7.6	-35.42	Tyr355, Met522, Ile523
11	-8.0	-33.23	Met522
Flurbiprofen ^a	-8.8	-38.21	Arg120, Tyr355

^aCo-crystallized ligand

Table 6. COX-2 1PXX binding affinities.

compound	Est. binding energy(kcal/mol)	Binding affinity score	RESIDUES of the active site participating in H-bonds
8	-8.2	-27.32	Gly526,Ser530
10	-8.8	-29.23	Tyr385, Met522
11	-9.6	-29.55	Ser530
diclofenac ^a	-9.0	-32.95	Tyr385, Ser530

^aCo-crystallized ligand

Interestingly, at COX-2 the NH group of the hydrazone is involved in an *intramolecular* H-bond to one of the phenol OHs.

Overall, the docking results indicate the potential of compounds **8**, **10** and **11** to exert their anti-inflammatory activity through COX-1/COX-2 inhibition.

2.2.2. Antioxidant Activity

Antioxidant activity of a structure is based on either its radical scavenging power or its Fe(II) chelating ability.^[70] A catechol-like substitution is known to be an ideal pattern for this type of activity.^[71] To scout the probability of a redox-triggered event related to the observed anti-inflammatory activity, some of our compounds were tested for possible antioxidant activity by the DPPH method (Table 4). Interestingly, apart from the parent **1**, which exhibited some activity, all the rest were found to be inactive.

2.3. Impact of Structure on its observed Biological Activity-Some Reflections

Looking at the anti-inflammatory profile (Table 4), we can deduce the following observations. Hydrazone **11** exhibits the best anti-inflammatory activity. Moreover, a comparison of the hydrazones **11–13**, reveals that the presence of the aryl group of the hydrazone arm contributes positively at the observed activity. The inhibitory potency of the tested oximes **8** and **10** does not seem to be influenced by the bromine substitution. Of the ketones **3** and **7**, it seems that the increased aromaticity of **7** with a potential to engage into arene-arene interactions has a positive impact at the inhibitory profile.

The formation of the pseudo ring H bridge reduces the flexibility and the hydrophilic character of the molecule. This is particularly observed in the case of **8** docked at COX-1 and **11** bound at COX-2.

No antioxidant activity has been demonstrated by the tested compounds, except for a rather low one displayed by the parent ketone **1** (Table 4).

Phenol is weakly acidic and a weak H donor, with a reported bond dissociation enthalpy (BDE) value of ca. 84–88 kcalmol⁻¹ [72], as is its benzophenone derivatives (pK_a < 9.5)^[73], whereas its oxidation-derived radical is strongly acidic and unstable (pK_a < 0). Oximes^[60] or hydrazones^[74] are also fairly acidic with a similar bond dissociation enthalpy (BDE) range of ca. 80–89 kcalmol⁻¹. It is known^[72] that an IHB stabilizes the phenol radical, lowers the BDE of the ring and subsequently lowers its redox potential. The position of OH in the ring, its efficient conjugation with it and a low BDE favour an effective radical scavenging capacity and ultimately antioxidant activity.^[75] It follows that a rather strong OH engagement in an IHB bridge, as in **1–6** or **8–13**, deprives the structure, at least in part, of its hydrophilic weaponry. This could decapacitate their radical scavenging-antioxidant activity, as it was confirmed experimentally.

Thus, having found a significant anti-inflammatory activity without any correlation with lipophilicity and no antioxidant activity in our structures, it appears that their anti-inflammatory response works through an intermolecular OH redox-controlled pathway or one via a metal chelation, perhaps. In this context, it may be argued that upon rotation about the 1(1')-7 bond of one of the rings, one (at least) OH group and the >C=X site are exposed to the surroundings, free to engage in *intermolecular* H (and/or other types of) bonding interactions (not excluding bifurcation of >C=X). Eventually, the receptor-ligand domain rearranges accordingly, reflecting the observed activity of our ligand structures. Thus, H bonding, as an arrested intermediate in a deprotonation event,^[76] could well be implicated by a PCET pathway,^[77,78] probably through solvent molecules.

Undoubtedly, the currently available data on the structure and anti-inflammatory profile of **1–13** pave the way to further investigations on a promising future for these structures. Accordingly, relevant work is intended in this context.

3. Conclusions

The current work applied DFT calculations, grid scan analysis and 2D ROESY-NMR spectroscopy towards the conformational analysis of the studied compounds. Parent **1** or di-substituted **4** display the possibility of unhindered rotation around the critical dihedrals τ_1 and τ_2 . Some of the favorable conformations feature the potential of a RAHB-assisted interaction. **3** and **5** seem to favour the formation of a bifurcated H-bridge. The oxime (**8–10**) or hydrazone (**11–13**) functionality introduces a steric hindrance, restricting the free rotation of the phenol rings. The H bridges are more tightly held in **1–6** compared to those in **8–13**. Their respective *pseudo* ring stabilities depend on the donor-acceptor power of the H bridge components and the ring size.

Some of the compounds showed significant anti-inflammatory activity, comparable to marketed drugs, the highest one observed for **11**. Our *in silico* studies proposed that their anti-inflammatory properties could be mediated through COX-

1/COX-2 enzymes. The binding modes of compounds **8**, and **11** could support the formation of pseudo ring H-bridges restraining their conformational flexibility and decreasing their hydrophilicity.

Supporting Information

Experimental and computational details, geometries, energetics, and aromaticities of the molecules, spectral data (1H NMR, mass spectroscopy, and IR) and docking studies have been provided in Supporting Information.

Acknowledgements

DT and IDP acknowledge financial support of this work by the General Secretariat for Research and Technology, Greece (project Polynano-Kripis 447963).

Keywords: 2,2'-Dihydroxybenzophenones · N-Carbonyl Derivatives · Synthesis · Anti-inflammatory Potential · DFT · NMR

- [1] A. de Meijere and F. Diederich in *Metal-Catalyzed Cross-Coupling Reactions*, 2nd ed.; John Wiley & Sons: Weinheim, Germany, **2004**.
- [2] S.-B. Wu, C. Long, E.J. Kennelly, *Nat. Prod. Rep.* **2014**, *31*, 1158–1174 and references cited therein.
- [3] D. Wang, R. DuBois, *Nat. Rev. Cancer*, **2010**, *10*, 181–193.
- [4] D. Diaz-Carballo, S. Malak, M. Freistuhler, A. Elmaagacli, W. Bardenheuer, H. P. Reusch, *Int. J. Clin. Pharmacol. Ther.* **2008**, *46*, 428–439.
- [5] B. Laursen, M.-P. Danieul, T. Skrydstrup, *Tetrahedron*, **2002**, *58*, 2231–2238.
- [6] G. Momekov, P.T. Nedialkov, G.M. Kitanov, D.Z. Zheleva-Dimitrova, T. Tzanova, U. Girreiser, M. Karaivanova, *Med. Chem.* **2006**, *2*, 377–384.
- [7] A. R. Katritzky, K. N. B. Le, P. P. Mohapatra, *Synthesis*, **2007**, 3141–3146.
- [8] L. H. Nguyen, G. Venkatraman, K. Y. Sim, L. J. Harrison, *Phytochemistry*, **2005**, *37*, 1718–1723.
- [9] U. M. Acuna, N. Jancovski, and E. J. Kenelly, *Curr. Top. Med. Chem.* **2013**, *9*, 1560–1580.
- [10] M. Zahedi-Tabrizi, S. F. Tayyari, F. Badalkhani-Kamseh, R. Ghomi, F. Afshar-Qahremani, *J. Chem. Sci.* **2014**, *126*, 919–929 and references cited therein.
- [11] C. Alvarez, R. Alvarez, P. Corchete, C. Pirez-Melero, R. Pelaez, M. Medarde, *Bioorg. Med. Chem.* **2008**, *16*, 8999–9008 and references cited therein.
- [12] J. P. Storm, C.-M. Andersson, *J. Org. Chem.* **2000**, *65*, 5264–5274 and references cited therein.
- [13] F. Kaiser, L. Schwink, J. Velder, H.-G. Schmalz, *J. Org. Chem.* **2002**, *67*, 9248–9256.
- [14] H. Kim, S. M. So, C. P.-H. Yen, E. Vinhato, A. J. Lough, J.-I. Hong, H.-J. Kim, and J. Chin, *Angew. Chem. Int. Ed.* **2008**, *47*, 8657–8660 and references cited therein.
- [15] R. Martin in *Aromatic Hydroxyketones: Preparation and Physical Properties* 3rd ed., Springer vol. 1, **2011**.
- [16] M. J. Romão, J. Knäblein, R. Huber, J. J. G. Moura, *Prog. Biophys. Mol. Biol.* **1997**, *68*, 121–144.
- [17] F. Minutolo, S. Bertini, A. Martinelli, G. Ortore, G. Placanica, G. Protta, S. Rapposelli, T. Tuccinardi, S. Sheng, K. E. Carlson, B. S. Katzenellenbogen, J. A. Katzenellenbogen, M. Macchia, *ARKIVOC*, **2006**, *viii*, 83–94 and references cited therein.
- [18] T. R. F. de Melo, R. C. Chelucci, M. E. L. Pires, L. A. Dutra, K. P. Barbieri, P. L. Bosquesi, G. H. G. Trossini, M. C. Chung, J. L. dos Santos, *Int. J. Mol. Sci.* **2014**, *15*, 5821–5837.
- [19] G. Verma, A. Marella, M. Shaquiquzaman, M. Akhtar, M. R. Ali, M. M. Alam, *J. Pharm. Bioallied Sci.* **2014**, *6*, 69–80.
- [20] S. A. Khanum, V. Girish, S. S. Suparshwa, N. F. Khanum, *Bioorg. Med. Chem. Lett.* **2009**, *19*, 1887–1891.
- [21] ADME(T): Absorption, Distribution, Metabolism, Excretion and Toxicity. These tests constitute a major protocol (known to be at the forefront of the drug design, discovery and development quest), to determine the efficacy of a drug candidate to proceed to Phase II trials (see J. P. Hughes, S. Rees, S. B. Kalindjian, and K. L. Philpott, *Br. J. Pharmacol.* **2011**, *162*, 1239–1249).
- [22] L. J. Marnett, *J. Org. Chem.* **2012**, *77*, 5224–5238 and references cited therein.
- [23] a) A. Kajal, S. Bala, N. Sharma, S. Kambij, V. Saini, *Int. J. Med. Chem.* **2014**, 761030, doi: 10.1155/2014/761030. b) R. W. Friesen, J. A. Mancini *Med. Chem.*, **2008**, *51*, 4059–4067. c) F. Medda, E. Sells, H.-H. Chang, J. Dietrich, S. Chappeta, B. Smith, V. Gokhale, E. J. Meuillet, C. Hulme *Bioorg. Med. Chem. Lett.*, **2013**, *23*, 528–531. d) B. Smith, H.-H. Chang, F. Medda, V. Gokhale, J. Dietrich, A. Davis, E. J. Meuillet, C. Hulme *Bioorg. Med. Chem. Lett.*, **2012**, *22*, 3567–3570.
- [24] S. A. Khanum, S. Shashikanth, A. V. Deepak, *Bioorg. Chem.* **2004**, *32*, 211–222.
- [25] Y. Gardikis, P. G. Tsoungas, C. Potamitis, M. Zervou, P. Cordopatis, *Heterocycles*, **2011**, *83*, 1077–1091 and 1291–1302.
- [26] M.-S. Seo, K. Kim, H. Kim, *Chem. Commun.* **2013**, 49, 11623–11625.
- [27] M. R. Odrowaz-Sypniewski, P. G. Tsoungas, G. Varvounis, P. Cordopatis, *Tetrahedron Lett.* **2009**, *50*, 5981–5983.
- [28] O. G. Zoi, T. N. Thireou, V. E. Rinotas, P. G. Tsoungas, E. E. Eliopoulos, E. K. Douni, N. E. Labrou, Y. D. Clonis, *J. Biomol. Screen.* **2013**, *18*, 1092–1102.
- [29] O. G. Zoi, T. N. Thireou, P. G. Tsoungas, E. E. Eliopoulos, N. E. Labrou, Y. D. Clonis, *Chem. Biol. Drug Des.* **2015**, accepted.
- [30] C. Tintori, F. Manetti, M. Botta, *Curr. Top. Med. Chem.* **2010**, *10*, 1019–1035.
- [31] F. Weng, C. Wang, B. Xu, *Tetrahedron Lett.* **2010**, *51*, 2593–2596.
- [32] E. Balali, A. Shamel, H. Naeimi, M. M. Ghambari, *Orient. J. Chem.* **2013**, *29*, 1611–1614 and references cited therein.
- [33] a) L. Skattebøl, T. V. Hansen, *Org. Synth.* **2012**, *89*, 220–229 and references cited therein. b) T. V. Hansen, L. Skattebøl, *Org. Synth.* **2005**, *82*, 64–68.
- [34] T. Leermann, F. R. Leroux, F. Colobert, *Org. Lett.* **2011**, *13*, 4479–4481.
- [35] G. Mora, S. Darses, J.-P. Genet, *Adv. Synth. Catal.* **2007**, *349*, 1180–1184.
- [36] C. Bolm, A. S. Magnus, J. P. Hildebrand, *Org. Lett.* **2000**, *2*, 1173–1175.
- [37] P. Gogoi, D. Konwar, *Org. Biomol. Chem.* **2005**, *3*, 3473–3475.
- [38] N. Mori, H. Togo, *Tetrahedron*, **2005**, *61*, 5915–5925.
- [39] A. Fürstner, H. Krause, *Adv. Synth. Catal.* **2001**, *343*, 343–350.
- [40] H. Zheng, Q. Zhang, J. Chen, M. Liu, S. Cheng, J. Ding, H. Wu, W. Su, *J. Org. Chem.* **2009**, *74*, 943–945.
- [41] S. Mondal, G. Panda, *RSC Adv.* **2014**, *4*, 28317–28358 and references cited therein.
- [42] Y. Zhao, V. Snieckus, *Org. Lett.* **2014**, *16*, 390–393.
- [43] N. Assimomytis, Y. Sariyannis, G. Stavropoulos, P. G. Tsoungas, G. Varvounis, P. Cordopatis, *Synlett.* **2009**, 2777–2782.
- [44] T. B. Nguyen, L. Ermolenko, M.-E. T. H. Dau, A. Al-Mourabit, *Heterocycles*, **2014**, *88*, 403–416.
- [45] J. W. Dankwardt, *J. Org. Chem.* **1998**, *63*, 3753–3755.
- [46] MgI₂ is usually effective in intramolecularly H bonded o-acyl phenols see: K. S. Lee, K. D. Kim, *Bull. Kor. Chem. Soc.* **2010**, *31*, 3842–3843 and references cited therein (see ref. 9 for the use of in situ prepared MgI₂ (OEt) 2).
- [47] P. Klán, T. Šolomek, C. G. Bochet, A. Blanc, R. Givens, M. Rubina, V. Popik, A. Kostikov, J. Wirz, *Chem. Rev.* **2013**, *113*, 119–191 and references therein.
- [48] B. Kuhn, P. Mohr, M. Stahl, *J. Med. Chem.* **2010**, *53*, 2601–2611.
- [49] N has an intrinsically higher PA than O, see: L. A. Reihardt, K. A. Sacksteder, W. W. Cleland, *J. Am. Chem. Soc.* **1998**, *120*, 13366–13369.
- [50] a) P. J. Cox, D. Kechagias, O. Kelly, *Acta Cryst.* **2008**, *B64*, 206–216. b) E. O. Schlemper, *Acta Cryst.* **1982**, *B38*, 1619–1622, and references cited therein.
- [51] G. Jaccard, J. Lauterwein, *Helv. Chim. Acta* **1986**, *69*, 1469–1485.
- [52] K. B. Andersen, M. Langgard, J. Spanget-Larsen, *J. Mol. Struct.* **1999**, *509*, 153–163.
- [53] L. Lu, L. He, *J. Mol. Struct.* **2012**, *1010*, 79–84.
- [54] R. D. Parra, K. Streu, *Comput. Theor. Chem.* **2011**, *977*, 181–187.

- [55] T. M. Krygowski, J. E. Zachara-Horeglad, M. Paluciak, *J. Org. Chem.* **2010**, *75*, 4944–4949 and references cited therein.
- [56] G. Gilli, P. Gilli in *The Nature of the Hydrogen Bond: Outline of a Comprehensive Hydrogen Bond Theory*, Oxford scholarship Monographs, 2009.
- [57] RAHBs are usually accompanied by notable changes in geometry or electronic properties reflected on further changes in critical points, corresponding to elongation of the X–H (X = proton donor) bond and shortening of the (X)H...Y (Y proton acceptor) bond within the H-bridge (see B. Bankiewicz, M. Palusiak, *Comput. Theor. Chem.* **2011**, *966*, 113–119).
- [58] Substituent constants σ have been measured for: $\sigma^+ = -0.18$ (Ph), $\sigma^+ = -0.17$ (Me) and $\sigma^- = -0.23$ (Br) [see K. C. Gross, P. G. Seybold, *Int. J. Quant. Chem.* **2001**, *95*, 569–579].
- [59] A. Nowroozi, H. Hajiabadi, *Struct. Chem.* **2014**, *25*, 215–220.
- [60] P. Politzer, J. S. Murray in *The Chemistry of Functional Groups*, Patai series, ed. Z. Rappoport, J.E. Liebman, Chapters 1 and 3, 2009, Wiley Interscience.
- [61] A. G. Smith, P. A. Tasker, D. J. White, *Coord. Chem. Rev.* **2003**, *241*, 61–85.
- [62] Van der Waals O and N radii are virtually equal (1.52 Å cf. 1.55 Å, see A. Bondi, *J. Phys. Chem.* **1964**, *68*, 441–451).
- [63] E. Buncel, I. H. Um, *Tetrahedron* **2004**, *60*, 7801–7825.
- [64] <http://www.ibmc.msk.ru/>; <http://www.pharmaexpert.ru/>.
- [65] V. V. Poroikov, D. A. Filimonov, W. D. Ihlenfeld, T. A. Glorizova, A. A. Lagunin, Yu. V. Borodina, A. V. Stepanchikova, M. C. Nicklaus, *J. Chem. Inf. Comput. Sci.* **2003**, *43*, 228–236.
- [66] V. Poroikov, D. Filimonov, in *Predictive Toxicology*, (Ed.: C. Helma) Taylor and Francis, **2005**, pp. 459–480.
- [67] E. T. Denisov, Igor B. Afanas'ev in *Oxidation and Antioxidants in Organic Chemistry & Biology*, Taylor & Francis, 2005.
- [68] B. S. Selinsky, K. Gupta, C. T. Sharkey, P. J. Loll, *Biochemistry* **2001**, *40*, 5172–5180.
- [69] S. W. Rowlinson, J. R. Kiefer, J. J. Prusakiewicz, J. L. Pawlitz, K. R. Kozak, A. S. Kalgutkar, W. C. Stallings, R. G. Kurumbail, L. J. Marnett, *J. Biol. Chem.* **2003**, *278*, 45763–45769.
- [70] M. Laguerre, J. Lecomte, P. Villeneuve, *Prog. Lipid Res.* **2007**, *46*, 244–282.
- [71] Lipophilic character and multiple sites of interaction determine ligand efficiency [see I. Jabeen, K. Pleban, U. Rinner, P. Chiba, G. F. Ecker, *J. Med. Chem.* **2012**, *55*, 3261–3278].
- [72] C. Aliaga, I. Almodovar, M. C. Rezende, *J. Mol. Model.* **2015**, *21*, 2572–2581.
- [73] G. T. Castro, S. E. Blanco, O. S. Giordano, *Molecules* **2000**, *5*, 426–427.
- [74] X. Su, I. Aprahamian, *Chem. Soc. Rev.* **2014**, *43*, 1963–1981 and references cited therein.
- [75] C. B. Aakeröy, S. Panikkattu, P. D. Chopade, J. Desper, *Cryst. Eng. Comm.* **2013**, *15*, 3125–3136.
- [76] A. P. Gamiz-Hernandez, A. Magomedov, G. Hummer, V. R. I. Kaila, *J. Phys. Chem. B* **2015**, *119*, 2611–2619.
- [77] J.-M. Savéant, *Ann. Rev. Anal. Chem.* **2014**, *7*, 537–560.
- [78] S. Hammes-Schiffer, *Energy Environ. Sci.* **2012**, *5*, 7696–7703.

Submitted: April 15, 2016

Accepted: June 13, 2016